

# New off-lattice Pattern Recognition Scheme for off-lattice kinetic Monte Carlo Simulations

Giridhar Nandipati, Abdelkader Kara, Syed Islamuddin Shah, Talat S. Rahman

*Department of Physics, University of Central Florida, Orlando, FL 32816*

---

## Abstract

We report the development of a new pattern-recognition scheme for the off-lattice self-learning kinetic Monte Carlo (KMC) method that is simple and flexible enough that it can be applied to all types of surfaces. In this scheme, to uniquely identify the local environment and associated processes involving three-dimensional (3D) motion of an atom or atoms, 3D space around a central atom or leading atom is divided into 3D rectangular boxes. The dimensions and the number of 3D boxes are determined by the type of the lattice and by the accuracy with which a process needs to be identified. As a test of this method we present the application of off-lattice KMC with the pattern-recognition scheme to 3D Cu island decay on the Cu(100) surface and to 2D diffusion of a Cu monomer and a dimer on the Cu (111) surface. We compare the results and computational efficiency to those available in the literature.

---

## 1. Introduction

Quantitative understanding of nucleation and growth of heteroepitaxial films is challenging from both fundamental and technological points of view, as these are important processes[1, 2, 3] for the fabrication of nanostructures ranging from quantum wires[4] to quantum dots.[5] Heteroepitaxial structures with

---

*Email addresses:* giridhar.nandipati@ucf.edu (Giridhar Nandipati), abdelkader.kara@ucf.edu (Abdelkader Kara), islamuddin@knights.ucf.edu (Syed Islamuddin Shah), talat.rahman@ucf.edu (Talat S. Rahman)

strained semi-conductor thin films have found wide application in electronic and optoelectronic devices.[6, 7] In many cases, the existence of strain due to lattice mismatch can lead to the formation of three dimensional (3D) clusters, [8, 9] whose shape can depends on variety of factors.

A common method for simulating heteroepitaxial growth is by applying molecular dynamics (MD) using many-body interaction potentials. In the MD method,[10, 11, 12] real motion of atoms is modeled through real-space integration of Newton's equations of motion, the forces acting upon each atom in the system are determined by the interatomic potentials for all atoms in the system. One of the main advantages of MD simulations is the explicit inclusion of system vibrational and thermal dynamics as controlled by the chosen interatomic potential. Together they allow the system to evolve freely (as a micro-canonical system) for timescales (a few hundred nanoseconds to microseconds) whose upper limit is imposed by available computational resources. MD simulations are in general limited to timescales of microseconds (the longest) that are still orders of magnitude smaller than those of experiments. Since typical experiments of interest (epitaxial growth, for example) report important morphological changes on timescales of minutes or hours, MD simulations may not be able to capture critical rare events and thereby fail to provide comprehensive evolution of the system.

Another method for studying epitaxial growth is to use kinetic Monte Carlo (KMC)[13, 14, 15, 16, 17, 18] simulations. It is extremely efficient for carrying out non-equilibrium simulations of dynamical processes when the relevant rates are known. As a result, the KMC method has been successfully used to carry out simulations of a wide variety of dynamical processes over experimentally relevant time and length scales. In KMC the thermal motion of the system is included only implicitly and in an approximate way. In KMC, rates of allowed processes, through which the system evolves, are provided as an input. If this input is accurate and complete, KMC simulations are in a good position to mimic experiments. One challenge is to determine as accurately as possible the parameters associated with these processes and, as completely as possible,

the full list of possible processes for the system. Another challenge with KMC method is that the systems investigated must be discretized and mapped onto a fixed lattice in order to define various diffusion mechanisms that must be considered at a given moment. Heteroepitaxial systems are thus especially hard to treat with KMC method because of the increased tendency for the system to go off-lattice, owing to strain due to lattice mismatch.

To address the problem of completeness, KMC methods have been developed that will find all the processes that can happen in the system on-the-fly,[19, 20, 21] removing the constraint that all the atomic-scale events have to be known *a priori*. One such method is the self-learning KMC (SLKMC) technique.[21] In SLKMC, a pattern-recognition scheme allows efficient storage and subsequent retrieval of information from a database of diffusion processes, their paths and their activation energy barriers. It has been used for detailed study of Ag island diffusion[21, 22] and of coarsening of Ag islands at late-stages [23] and early stages [24] on Ag(111) surface. This method is based on the assumption that all atoms sit on high-symmetry sites commensurate with the substrate (on-lattice sites) and are also at the same height. But for small clusters, atoms can sit on irregular atomic positions (off-lattice sites) even in homoepitaxial systems[25] and this behavior is even more frequent for heteroepitaxial systems, in which atoms for islands of all sizes may occupy ‘off-lattice’ sites. To describe these systems, a pattern-recognition scheme is required in which atoms are allowed to be at any position on the surface. In an effort to overcome this problem Kara *et al* [25] developed two-dimensional (2D) off-lattice pattern recognition scheme and used it to study heteroepitaxial island diffusion. Since the pattern-recognition scheme mentioned above can capture only 2D diffusion processes, a new pattern recognition technique is needed to model 3D motion of an atom. In this article we present a new off-lattice pattern-recognition scheme that can recognize three-dimensional (3D) processes and is flexible enough to be applied to all types of lattices. Although our original goal of off-lattice KMC method was to use it to study heteroepitaxial systems, in this article we test it by studying 2D diffusivity of Cu island on Cu(111) surface and decay of 3D Cu islands on

Cu(100) and compare the results with those of previous studies.

The organization of this paper is as follows. In section 2 we give a very brief description of SLKMC algorithm. In section 3 we discuss the need for a new pattern recognition scheme and describe in detail our implementation of the new 3D off-lattice pattern-recognition scheme. In section 5, as a test of our scheme we present results for diffusivity of a Cu monomer and a dimer on Cu(111) surface and for 3D Cu island decay on Cu(100) surface, and compare these with those of previously reported. Concluding remarks are presented in section 6.

## 2. Self-Learning kinetic Monte Carlo Algorithm

In on-the-fly KMC simulations, instead of using a fixed set of diffusion processes each with its activation barriers, all the possible diffusion processes are determined at each KMC step. In contrast, in SLKMC the usage of a pattern-recognition scheme gives the ability to determine whether the energetics of all the possible processes have been determined and stored in a database during the course of a simulation. If all the possible processes are stored in the database, no further action is taken, and the KMC simulation continues its course as in standard KMC with a complete list of processes. But whenever a new configuration is found, all its possible diffusion processes and their respective activation barriers are determined by saddle-point searches. The new configuration, together with its associated diffusion processes (each with its activation barriers) is stored in a database. Every new simulation starts from an empty database and gets filled up with new configurations and associated processes as it proceeds, until all the possible processes that can happen in the system are found.

Several methods can be used to do saddle-point search. A simple one is called the “drag method”, in which an atom is dragged in the direction of the nearest vacant site in small steps. During the process all the atoms in the model system are allowed to relax in all directions, except for the diffusion atom which is allowed to relax only in the directions normal to that along which it is ‘dragged’.

This prevents the atom moving back to the initial state. This method is efficient and easy to implement.

### 3. Two Dimensional Pattern Recognition Scheme

As mentioned earlier, in KMC method we need to know all the processes possible. Each process involves some particular motion of an atom (or atoms) and whose activation barrier depend on the local neighborhood. In order to uniquely identify the local neighborhood and the diffusion processes associated with, and to store and retrieve this information on the fly, a pattern recognition-scheme is necessary. Storing and retrieving this information avoids redundancy, as the system “learns” from its “past,” that is, from its memory of the processes and their energetics associated with previously encountered patterns (or configurations). For this to succeed a pattern recognition scheme must be accurate enough to uniquely distinguish different shapes in the system as they appear and make decisions using information already stored.

One of the first pattern-recognition schemes [21] developed was to model on-lattice 2D diffusion of atoms on a (111) surface (it can be easily extended to other types of surfaces). In this scheme, neighboring fcc sites around a central atom are grouped into rings and depending on occupancy of fcc sites in these rings a decimal integer can be generated that uniquely identifies the neighborhood around the central or leading atom. Though very simple and easy to implement this pattern recognition scheme cannot accommodate systems in which an atom sits at an hcp sites or a non-symmetry(off-lattice) positions due to lattice mis-match. To allow for off-lattice sites, a new pattern recognition scheme [25] was developed to handle 2D diffusion of clusters on (111) surfaces (it too can be easily extended to other types of surfaces). In this scheme, a set of relative positions of atoms with respect to a chosen ‘reference point’ is used to identify a local neighborhood around a leading or central atom. For the fcc (111) surface, the reference point is either (1) a fcc or hcp site closest to the ‘leading atom’ (any atom in the system can be selected as the leading atom) in the cluster or (2) a fcc or hcp site closest to the center of mass of

the cluster. Every atom in the cluster then has uniquely defined coordinates with respect to this reference site. Instead of an integer configuration key, each atom's coordinates with respect to the reference site are stored in the database along with each of its possible diffusion processes and their respective activation barrier. We note that these distance are not stored in any particular order in the database.

Although the latter method of classifying the neighborhoods removes restriction to on-lattice systems, one of its main disadvantages is that the identification of pattern involves matching non-integer distances of atoms in the simulation with those in the database. Tolerance for matching these real (non-integer) numbers becomes very important: if the tolerance is small, the database will be very large (with the result that configurations might be redundant); if it is large, a valid configuration might not be identified as unique. In the database each configuration is shape of an island identified by relative distances of each atom with respect to chosen reference point (either fcc or hcp site), to which all the possible processes and their activation barriers are attached. Pattern recognition involves matching relative distances of all the atoms in a cluster with those stored in the database, this increases computational effort with increasing cluster size. For an unsorted database, which usually is the case, computational effort increases linearly as number of the configurations. While for a configuration with an unsorted list of distances, computational effort for matching distances of each individual atom in the cluster increases as square of number of atom in the cluster. For example, for an  $N$  atom cluster to match the coordinates of first atom simulation does  $N$  searches, then for the second atom it is  $(N-1)$  searches and so on. Therefore computational effort in matching a pattern approximately increases as  $N^2/2$  with the cluster size

#### **4. Three-dimensional off-lattice pattern recognition scheme**

To overcome the short comings of previously developed pattern recognition schemes, a new scheme is needed which, apart from being applicable to off-lattice systems, should have following properties: (1) pattern matching should



Figure 1: 3D space is split up into 3D boxes with central or leading atom at the center of the middle box.

be based on integers which identifies the neighborhood of a central atom; (2) it should be flexible enough to be applicable to all lattice types and; (3) it should be able to handle both 2D and 3D diffusion processes. In the new scheme developed here, 3D space around the central atom is divided into rectangular boxes of appropriate size as shown in Fig. 1 which looks like a Rubik's cube from the outside. The size of "super box" (the blue box in Fig 2) which encloses the smaller rectangular boxes (we call them simply "boxes") is dependent on the range of interaction in the system being studied. We note that the neighborhood of every atom in the system is identified by treating it as a "central atom". The entire system of boxes is designed so that this central atom is always at the center of the middle box; thus the middle box is always occupied while the neighboring atoms are assigned to a given box if its center of mass lies within the box, allowing them to be anywhere within a box. Based on the occupancy of the constituent boxes a unique binary number is generated to identify a particular neighborhood around the central atom.

#### 4.1. Implementation

In this article we use the fcc(100) surface to fully describe the implementation of our pattern recognition scheme. Figs 2(a) &(b) shows the top and side views of a 3D box system. The idea is very simple: a 3D box is constructed around the central atom symmetrically, whose dimensions depend on the range of the interaction for the system under study. Let us imagine the blue box as a 3D box around the central atom (blue colored atom in fig. 2), which is at the center

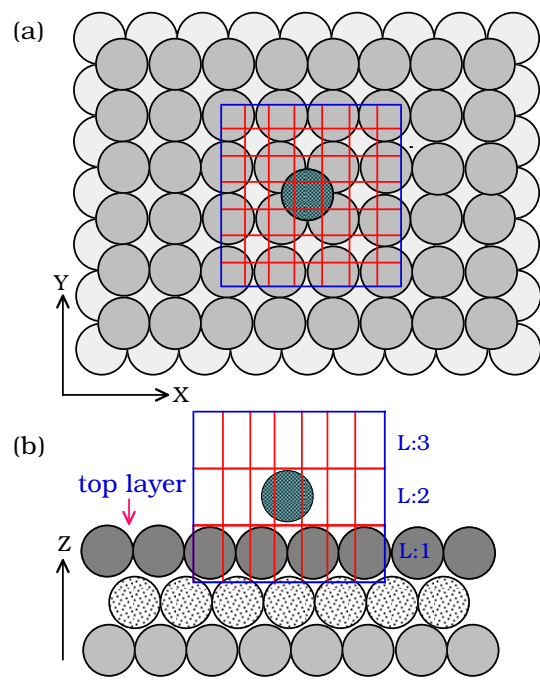


Figure 2: Monomer on fcc (100) surface (a) top view (b) side view. Bigger box (blue) is called the 'super box' ; smaller ones are called just boxes or smaller boxes. L1, L2, L3 are layers



of this 3D box and we call this box the “super box”. This super box is further divided into equal-sized smaller boxes. Division of the super box into smaller boxes is done in such a way that all boxes are distributed symmetrically around the central atom, assuring that it is always at the center of the middlemost box. These smaller boxes do not need to have same dimensions in x, y, & z directions. But dimensions of all smaller rectangular boxes are kept the same and depends on precision with which a process needs to be identified. Neighboring atoms are assigned to one of these smaller boxes based on whether its center of mass falls within the box. Unlike the central atom which has the restriction of being always at the center of the middlemost box, neighboring atoms can be anywhere within the box and only one atom is allowed in each box. A binary number is generated based on the occupancy (1 for occupied and 0 for unoccupied) which is converted to a decimal and stored in a database along with the information of all possible processes and their activation barriers, which we will discuss next in detail.

For the case of fcc (100) surface the size of the super box is chosen to include at least 3 layers of atoms (see fig. 2(b)), a substrate layer  $L1$  and adsorbate layers  $L2$  &  $L3$ . Depending on whether the system being studied is 2D or 3D, layer  $L3$  will be either empty or occupied. Thus, super box is divided to  $7 \times 7 \times 3$  smaller boxes in x, y & z directions respectively, which corresponds to 49 boxes in each of the layer (x-y plane), and a total of 147 boxes in 3 layers. These numbers can be adjusted according to need. To uniquely identify the 3D neighborhood a binary number can be generated based on the occupancy of the boxes. For a 147-box system it will be a 147-bit binary number, which is too large to handle. This binary number is thus split into 49 bit numbers which represent occupancy of boxes in each of the three layers. Thus, the 3D neighborhood around a central atom is uniquely represented by 3 decimal integer numbers and we call them ‘layer numbers’. As mentioned earlier, the number of these small boxes is an adjustable parameter. As can be seen in fig. 2, the height of the small box has been set equal to the interlayer spacing while the width and length are set as half the nearest neighbor distance, sufficiently small to accurately distinguish

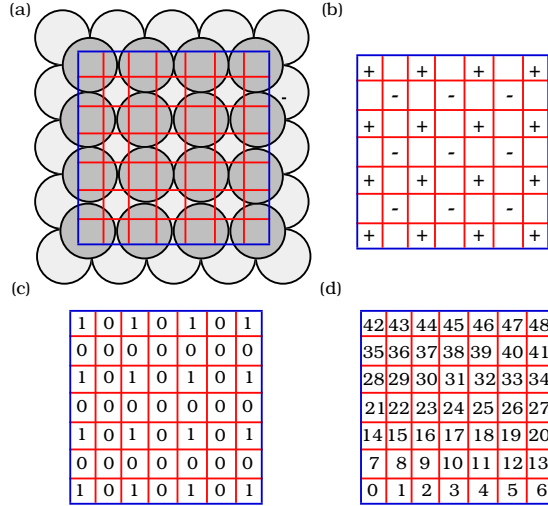


Figure 3: Shows generation of a binary number for the substrate layer ( $L_1$ ). (a) top view of boxes in substrate layer (b) sign '+' represents presence of substrate atom, '-' represents four-fold hollow site and empty box represent bridge sites (c) shows 0's and 1's for the substrate sites (d) ordering of binary digits

among 4-fold, hollow, bridge and A-top sites.

To generate the binary number which uniquely identifies the 3D neighborhood around the central atom, boxes that are filled by the neighborhood atoms are identified and are assigned 1's while rest of the boxes are assigned zeros. Fig. 3 shows the generation of a layer number for the substrate layer ( $L_1$ ). By comparing figs. 3(a) & (b) it can be seen that box with '+' represents box with the substrate atoms, '-' represents boxes with four-fold hollow sites and empty boxes represent bridge sites. All boxes, except the ones with '+' sign, are empty. Accordingly fig. 3(c) shows 1's and 0's based on the occupancy of the boxes for the the substrate atoms. Digits of the binary number in each layer are read starting from box No: 0 to box no: 48 as shown in fig 3(d). For the substrate layer  $L_1$  (dark-colored circles) shown in fig 2(a), layer number is equal to  $2^0 + 2^2 + 2^4 + 2^6 + 2^{14} + 2^{16} + 2^{18} + 2^{20} + 2^{28} + 2^{30} + 2^{32} + 2^{34} + 2^{42} + 2^{44} + 2^{46} + 2^{48} = 373856771850325$ . While for the case of an atom (green colored circle) in a tetramer in fig. 4(a) in the layer  $L_2$ , layer number is equal to  $2^{24} + 2^{26} + 2^{38} + 2^{40} = 13744734208000$  (compare figs. 4(b) & 3(d)) and for

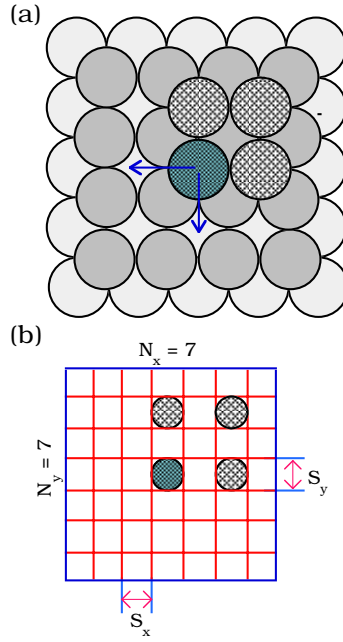


Figure 4: (a) Tetramer on a fcc(100) surface. Green colored circle repents the central atom. (b) location of atoms in the box system in layer  $L2$

the empty third layer( $L3$ ) it is zero. These three numbers are then stored in the database in a pre determined format which we will discuss it later in section 4.2

To implement this method all that is necessary is a way to identify the number of the box where the neighboring atom is located. A method can be easily developed to extract the box numbers of the neighboring atoms from their positions relative to the leading or central atom. Fig. 5 shows the sequential numbering of smaller boxes starting for the bottom two layer( $L1$  &  $L2$ ) for the purpose of their identification. Numbering of boxes starts from the left corner box (box no: 0 in fig 5) in the bottom most layer, which is  $L1$  and continues sequentially to the right corner box (box no: 146 (not shown)) in the third layer  $L3$ . Each small box is given integer coordinates with Box No:0 being the origin. Box No:0 has integer coordinates of  $(0, 0, 0)$ , similarly integer coordinates of Box No: 73, which hold the central atom for the present case, are  $(3, 3, 1)$ . If  $x_c, y_c$  &  $z_c$  are real coordinates of central atom and  $x_n, y_n$  &  $z_n$  are the real coordinates

91	92	93	94	95	96	97
84	85	86	87	88	89	90
77	78	79	80	81	82	83
70	71	72	73	74	75	76
63	64	65	66	67	68	69
56	57	58	59	60	61	62
49	50	51	52	53	54	55
42	43	44	45	46	47	48
35	36	37	38	39	40	41
28	29	30	31	32	33	34
21	22	23	24	25	26	27
14	15	16	17	18	19	20
7	8	9	10	11	12	13
0	1	2	3	4	5	6

Figure 5: Numbering of smaller boxes in the first two layers. Box with blue circle is the location of leading atom

of neighboring atom then integer coordinates can be obtained for the relative distances of neighboring atoms in real coordinates with respect to the central atom using following simple equations.

$$i = \left(\frac{x_r}{s_x}\right)_I + \left(\frac{N_x}{2}\right)_I \quad x_r = x_c - x_n \quad (1)$$

$$j = \left(\frac{y_r}{s_y}\right)_I + \left(\frac{N_y}{2}\right)_I \quad y_r = y_c - y_n \quad (2)$$

$$k = \left(\frac{z_r}{s_z}\right)_I + \left(\frac{N_z}{2}\right)_I \quad z_r = z_c - z_n \quad (3)$$

$()_I$  represents *integer division* in which fractional part or remainder is discarded.  $x_r, y_r, z_r$  are real coordinates of a particular neighboring atom relative to the leading atom, i.e., the difference in the  $x, y$  &  $z$  coordinates of leading atom and those of neighboring atom. While  $s_x, s_y$  &  $s_z$  (see fig. 4(b)) are real dimensions of a smaller box and  $N_x, N_y$  &  $N_z$  are number of small boxes in  $x, y$  &  $z$  directions respectively; then  $i, j$ , and  $k$  are integer coordinates of the small box in which

that neighboring atom is located with Box. No.0 being the origin. Since our super box is divided into  $7 \times 7 \times 3$  smaller boxes  $N_x = 7$ ,  $N_y = 7$  &  $N_z = 3$  as shown in fig. 4(b). While  $S_x = 1.28\text{\AA}$ ,  $S_y = 1.28\text{\AA}$  and  $S_z = 2.08\text{\AA}$  for the case of Cu (100) surface. Note that, if we know the integer coordinates of a box with respect to Box No. 0 then its box number is given as

$$\text{Box Number} = i + j * N_x + k * (N_x * N_y) \quad (4)$$

By following this method of checking the neighborhood within the range of interaction one can obtain the list of occupied boxes, there by generating a decimal number that identifies the neighborhood uniquely.

Unlike on-lattice KMC simulation, in an off-lattice KMC in order to identify the neighborhood of any atom efficiently, a neighborhood list is required. To do this we divide the system into equal-sized cells whose dimensions are larger than the range of interaction and a list of all atoms within that cell is maintained, similar to molecular dynamics (MD) simulations.[32] To identify the neighborhood of an atom all the atoms within the cell where this atom is located are checked, instead of the entire system. In order to take care of situations where an atom is near a cell boundary, list also includes information about atoms from the adjacent cells that are within a distance of half the cell size.

#### 4.2. Database

As mentioned earlier, in the original SLKMC, in the three-ring format, three integers were used to determine a given configuration. Similarly in the present database, three integer layer number are used to determine the configuration. Fig. 6 shows the format how each configuration and associated processes are stored in the database. The configuration shown fig. 6(a) is for a central atom (green circle in fig. 4(a)) in a tetramer on a fcc(100) surface while configuration shown in fig. 6(b) is for an atom in a dimer with both atoms on fcc sites on a fcc (111) surface. In fig. 6(a), the first three numbers (inside red circle) represent layer number for each of the three layers. The next number (inside blue circle) of processes possible for that configuration. Individual processes are

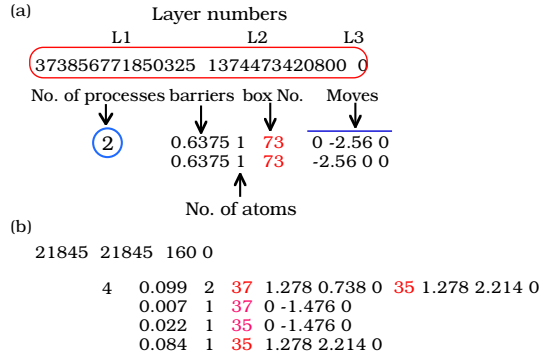


Figure 6: Format of the database (a) configuration for an atom in a tetramer (fig. 4) on fcc(100) surface (b) configuration an atom in a dimer on a fcc(111) surface.

represent by their activation barrier, number of atoms involved in the process, box numbers (colored red) of those atoms and their displacements in x, y & z directions. For fcc(111) surface we used four layer numbers to identify the configuration which includes layers below the central atom and one layer above it. We note that while pattern-recognition acts upon integers instead of real numbers the actual motion of the atoms are described in real numbers, which are displacements coordinates from the current coordinated of the adatoms.

In order to minimize the size of the database, symmetry of the type of the lattice under study can be used. For the case of fcc(100) surface we used (1)  $90^\circ$  rotation (2)  $180^\circ$  rotation (3)  $270^\circ$  rotation (4) mirror reflection (5) mirror reflection followed by  $90^\circ$  rotation (6) mirror reflection followed by  $180^\circ$  rotation (7) mirror reflection followed by  $270^\circ$  rotation. Thus, if a given configuration was not found in the database, then symmetry operations were performed to find symmetric configurations and a new search is done to find to see if it exists in the database. Instead of performing them when required, alternatively symmetric configurations can also be found ahead of time and stored in the memory during the simulation.

Every time an unknown configuration, which represents a local neighborhood not previously encountered, is found, then symmetry operations are performed and database is searched. If it is still not found then a saddle point search is

done to find all the possible processes. This new configuration is then appended to the existing database and corresponding rate tables in the simulation are updated accordingly. Thus an empty database is filled up with configurations as they appear during the course of the simulation and accumulation of this database does not proceed uniformly with time.[21] In a saddle point search, positions of all the neighboring atoms in real coordinates with respect to the central atom that could affect its motion are included. If the configuration of a central atom is unknown then there is always a possibility that configurations of its neighboring atoms are also unknown, resulting in saddle point searches for more than one atom. The size of the database usually depends on the system, range of interaction (or size of the super box), and accuracy (or size of the small box) with which a process needs to be identified.

## 5. Results

As mentioned earlier that the idea of developing this new pattern recognition is to be able to do simulations where atoms can go off-lattice and not sit on symmetric sites. As a first application or rather as a test we would study homoepitaxial systems, where atoms move from one symmetric position to another. But, the division of 3D space does allow the atom to move to an off-lattice location. In this article we examine the decay of 3D Cu islands on Cu(100) surface and compare results to the existing results in the literature. Also in order to show that the 3D pattern-recognition scheme is applicable to all types of lattices, we apply it to simulate 2D diffusion of Cu monomer and dimer on Cu(111).

### 5.1. Decay of Cu 3D islands on Cu(100) surface

In these simulations we have used a single fcc(100) substrate with periodic boundary conditions in the x-y plane (parallel to the surface). 3D islands of various sizes are created manually on this substrate, and they have a four-sided pyramidal shape with (111) facets (Fig. 7 shows a 3D island of size 29 atoms). The decay of these islands is simulated until the entire island reduces to a

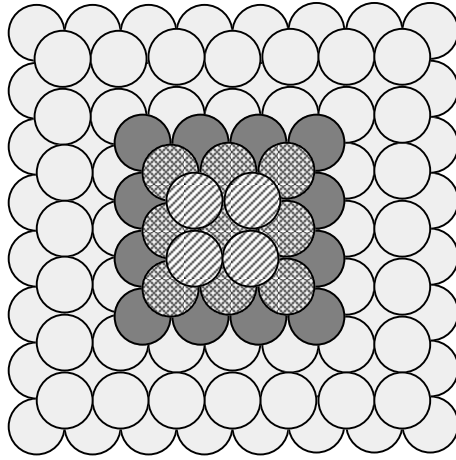


Figure 7: Nano-cluster 29 atoms

monolayer and this decay is studied as a function of temperature and 3D island size. The size of the substrate is  $125.44 \times 125.44 \text{ \AA}$  or  $50 \times 50$  lattice units.

Since the objective was to test the new pattern recognition scheme, to save time we used energy barriers based on parameterization of EMT barriers calculated by Jacobsen [31] for Cu island decay on Cu(100). For this case, every time there is a new configuration, possible processes and their diffusion barriers are found using the parameterization and are saved in the database. To take into account the Ehrlich-Schwoebel (ES) barrier to interlayer diffusion,[33, 34] for all interlayer diffusion processes an additional barrier of 0.02 eV is added to the values of the intra-layer diffusion barrier. These simulations also include downward funneling (DF),[35] for atoms at non-four-fold hollow sites. Atoms at these sites “cascade” randomly until they find a four-fold hollow site. At the temperatures we examined, this is a non-activated process. Since these simulations are SLKMC simulations, whenever a new configurations is found, all the possible processes and their barriers are found using the above mentioned EMT parameterization, and stored in the database. The size of the accumulated database is around 650 configurations depending on the size of the cluster.

Figure 8 shows the time that is required for 3D islands of sizes 45, 91 and 168 atoms to decay to one monolayer at various temperatures. Because the decay



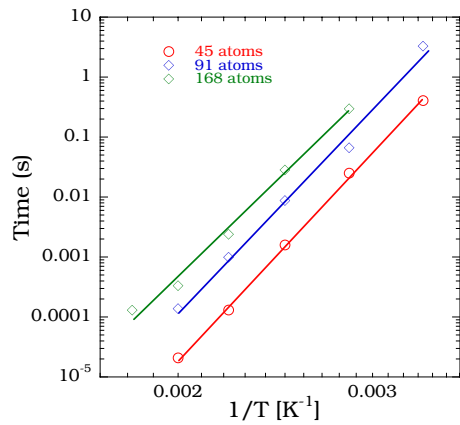


Figure 8: The time required for the reduction of 3D nano-clusters to one monolayer for clusters of sizes 45, 91 and 168 atoms at different temperatures. The lines have been fitted to the data assuming an Arrhenius behavior.

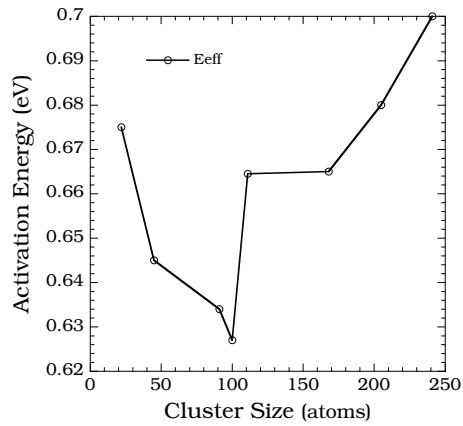


Figure 9: The effective activation energy as a function of the cluster size (atoms). This is an effective activation barrier for a 3D cluster to decay to a one monolayer of atoms. Obtained by fitting the data assuming an Arrhenius behavior.

process has Arrhenius behavior, effective activation barriers can be calculated by fitting the data to a straight line. Fig. 9 shows the plot of the effective activation barrier as a function of 3D cluster size with a minimum at 100 atom cluster and is in agreement with previous published results.[36]

### 5.2. 2D diffusion on Cu(111) surface

The 3D pattern-recognition scheme uses 3D rectangular boxes commensurate with the fcc(100) lattice, which has a square symmetry. To show that this pattern-recognition scheme can be applied to any type of lattice we have also studied 2D diffusion on fcc(111) surface, which is a triangular symmetry. Database of processes for Cu(111) island diffusion were obtained by using the drag method and were checked against the barrier calculated using the more sophisticated nudged-elastic band (NEB) method. The interatomic potentials were modeled using the embedded-atom method.[26] A simplification was introduced by assuming a ‘normal’ value for all diffusion prefactors, although we are aware that multi-atom processes may be characterized by high prefactors.[27, 28, 29, 30]

In these simulations we have a two-layer fcc(111) substrate with periodic boundary conditions in x-y plane (parallel to the surface) and adatom island is placed on top of the substrate. For fcc (111) surface four layers are used for pattern recognition. These simulations were performed for about  $10^7$  KMC steps at 300, 400, 500 and 700 K. During each simulation, the position of the center of mass was recorded after every 1000 KMC steps. The diffusion coefficient  $D$  of an adatom island for a 2D random walk was calculated using Einstein Equation:[37]  $D = \lim_{t \rightarrow \infty} \langle R_{CM}(t) - R_{CM}(0) \rangle^2 / 2dt$ , where  $R_{CM}(t)$  is the position of the center of mass of the island at time  $t$ , and  $d$  is the dimensionality of the system. Also, effective diffusion barriers are extracted for monomer and dimer from Arrhenius plot of  $\ln D$  Vs  $1/k_B T$ . The goal is to test the new pattern-recognition scheme by comparing calculated diffusion coefficients and effective energy barriers with already published values.[22]

In Fig. 10, we show the trace of the position of the center of mass on the (x,

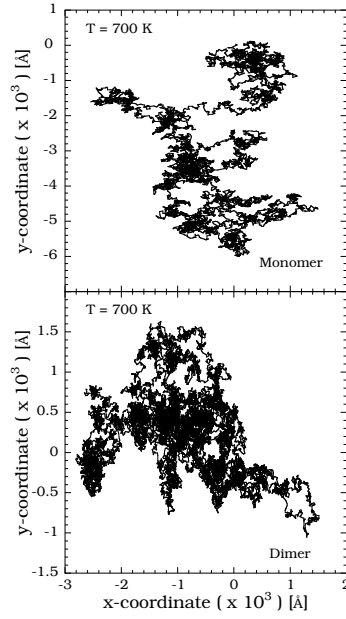


Figure 10: Trace of the center of mass of Cu monomer and dimer on Cu(111) at 700 K

Table 1: Diffusion coefficient for Cu monomer and dimer on Cu(111) ( $\text{\AA}^2/\text{s}$ )

Cluster Size	300 K	500 K	700 K
Monomer	$4.8 \times 10^{11}$	$8.2 \times 10^{11}$	$9.2 \times 10^{11}$
Dimer	$1.1 \times 10^{11}$	$4.2 \times 10^{11}$	$7.2 \times 10^{11}$

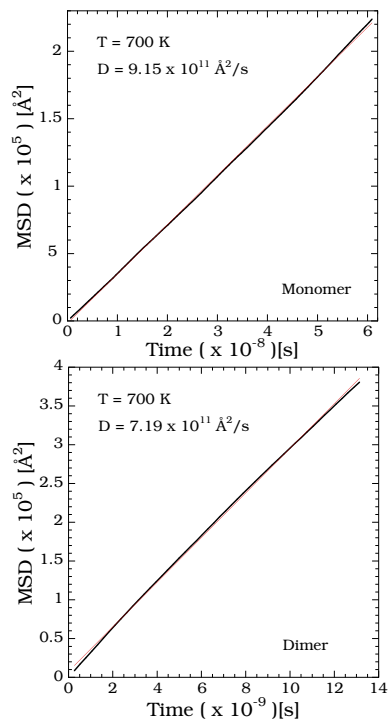


Figure 11: Mean square displacement (MSD) for Cu monomer and dimer on Cu(111) as a function of time at 700 K

y) plane for both monomer and dimer at 700 K after every 1000 KMC steps. The corresponding mean square displacements, for both monomer and dimer, as a function of time show a linear behavior (within statistical error) and are shown in fig. 11. The slope extracted from the mean square displacement plot reduced by 4 gives the diffusion coefficient. Table 1 shows the diffusion coefficients of monomer and dimer at 4 different temperatures. The effective barriers extracted from the Arrhenius plot for the monomer and dimer are 0.029eV and 0.083eV, respectively. These values are within the statistical error of already published results [22] shows that pattern recognition scheme works well with 2D diffusion.

## 6. Discussion

In order to overcome the short comings of previously developed pattern recognition schemes used to identify the local neighborhoods and to accurately account for different types of 2D and 3D diffusion processes, which might involve atoms moving to either symmetric or non-symmetric (off-lattice) sites, we have developed a new 3D off-lattice pattern recognition scheme. This new pattern recognition scheme is simple, flexible and allows identification of local neighborhoods more accurately. The accuracy of pattern recognition comes from the fact that it changes the pattern-recognition from the matching of real number to integers. The flexibility lies in fact that it can be extended to simulate 3D systems very easily and also different types of lattice without significant change to the simulation code. We note that this pattern recognition can be very easily adapted for on-lattice simulations, thus allowing for the identification of processes involving 3D motion of an atom or atoms.

We have tested this method by studying 2D diffusivity of Cu islands on Cu (111) surface and decay of Cu 3D islands on Cu(100) surface and comparing the results with those are available in the literature. Even though the processes allowed in these simulations move the atoms from one symmetric site to another pattern recognition allows the identification of neighborhood and corresponding processes if atoms sites at a non-symmetric or off-lattice sites. It can be seen

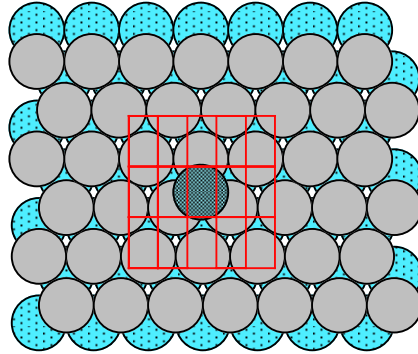


Figure 12: Monomer (dark blue atom) on a fcc site on fcc (111) surface. Shows division of space on the third layer  $L3$ .

from the fig. 3 that the division of 3D space allows the identification of 4-fold hollow site, A-top site and bridge site on layer  $L2$ . For fcc (111) surface four layers, two substrate layers and two adatom layers, are used for pattern recognition. Fig. 12 shows division of space for the third layer ( $L3$ ) adatom layer, it can be seen that the size of the smaller box used is accurate enough for the identification of both fcc and hcp sites. This is because in our simulations we only allowed atoms to move from one symmetric site to another. It can also be seen from the picture that size of the super box is large enough to include one ring from the ring-based pattern recognition scheme. But, the size of the small box can be easily reduced, thereby increasing number of small boxes, to make the recognition even finer allowing the identification of atoms which sit on off-lattice sites.

As mentioned earlier in the article, the accuracy with which a process is identified depends on the size of the small box. The size of the small box should be small enough it only allows only one atom in each box and that displacement of atoms moves them from one box to another. Thus, the tolerance for this new method is the dimensions of the small box. We note that some knowledge about the system under study is needed to determine not only the size of the super box but also the dimensions of small box. Also for a fixed size of a super box the computational effort in identifying a pattern does not vary much with

the dimensions of the small box, but increases with increasing size of the super box. This is because the computational effort in searching the neighborhood is independent of the size of the small box.

Motivation behind developing this pattern recognition scheme is to improve upon previously developed schemes. This method is computationally more expensive compared to previous methods but gives greater flexibility and extends the range of types of systems that can be simulated using KMC method. We note for the case of 2D diffusion on fcc (111) surface each KMC step takes in the order of couple of micro-seconds depending on the computing speed of the processor. On a Intel Core 2 Duo 2.26 GHz machine, each KMC step takes about 2.2ms. These type of simulations are excellent candidates for parallel simulations. This 3D pattern recognition scheme might be useful in simulation studies of morphological evolution of metal surfaces and in further development in KMC simulations of thin film growth.

## 7. Acknowledgement

This work was supported by NSF-ITR grant no. 0840389. We would also like to acknowledge of the support of computational resources of University of Central Florida (STOKES) and also grant of computer time from TeraGrid (TG-DMR110046). We thank Lyman Baker for critical reading of the manuscript.

## References

- [1] Y. Saito, Statistical Physics of Crystal Growth, World Scientific, Singapore, 1996.
- [2] R. Nötzel, J. Temmyo, T. Tamamura, Nature 369.
- [3] R. Jullien, J. Kertesz, P. Meakin, D. E. Wolf, Surface Disordering: Growth, Roughening and Phase Transitions, Nova, Commack, New York, 1993.
- [4] M. Notomi, J. Hammersberg, H. Weman, S. Nojima, H. Sugiura, M. Okamoto, T. Tamamura, M. Potemski, Phys. Rev. B 52 (1995) 11147.

- [5] J. L. Gray, N. Singh, D. M. Elzey, R. Hull, J. A. Floro, Phys. Rev. Lett. 92 (2004) 135504.
- [6] P. Kordos, J. Novak (Eds.), Heterostructure Epitaxy and Devices, Boston: Kluwer, 1998.
- [7] T. P. Pearsall (Ed.), Strain Layer Super-lattices, Boston: Academic, 1990.
- [8] Y. W. Mo, D. E. Savage, B. S. Swartzentruber, M. G. Lagally, Phys. Rev. Lett. 65 (1990) 1020.
- [9] D. J. Eaglesham, M. Cerullo, Phys. Rev. Lett 64 (1990) 1943.
- [10] M. Schneider, A. Rahman, I. K. Schuller, Phys. Rev. Lett. 55 (1985) 604.
- [11] B. W. Dodson, CRC Crit. Rev. Solid. State Mater. Sci 16 (1990) 115.
- [12] M. Schneider, I. Schuller, A. Rahman, Phys. Rev. B 36 (1987) 1340.
- [13] A. B. Bortz, M. H. Kalos, J. L. Lebowitz, J. Comput. Phys. 17 (1975) 10.
- [14] G. H. Gilmer, J. Crystal. Growth. 35 (1976) 15.
- [15] A. F. Voter, Phys. Rev. B 34 (1986) 6819.
- [16] P. A. Maksym, Semiconf. Sci. Technol. 3 (1988) 594.
- [17] K. A. Fichthorn, W. H. Weinberg, J. Chem. Phys. 95 (1991) 1090.
- [18] J. L. Blue, I. Beichl, F. Sullivan, Phys. Rev. E 51 (1995) R867.
- [19] G. M. H. Jónsson, K. W. Jacobsen, Classical and Quantum Dynamics in Condensed Phase Simulations, World Scientific, Singapore, 1998.
- [20] G. Henkelman, H. Jonsson, J. Chem. Phys. 115 (2001) 9657.
- [21] O. Trushin, A. Karim, A. Kara, T. S. Rahman, Phys. Rev. B 72 (2005) 115401.
- [22] A. Karim, A. N. Al-Rawi, A. Kara, T. S. Rahman, O. Trushin, T. Ala-Nissila, Phys. Rev. B 73 (2006) 165411.



- [23] G. Nandipati, Y. Shim, J. G. Amar, A. Karim, A. Kara, T. S. Rahman, O. Trushin, *J. Phys.: Condens. Matter* 21 (084214).
- [24] G. Nandipati, A. Kara, S. I. Shah, T. S. Rahman, *J. Phys.: Condens. Matter* 23 (2011) 262001.
- [25] A. Kara, O. Trushin, H. Yildirim, T. S. Rahman, *J. Phys.: Condens. Matter* 21.
- [26] S. M. Foiles, M. I. Baskes, M. S. Daw, *Phys. Rev. B* 33 (1986) 7983.
- [27] H. Yildirim, A. Kara, S. Durukanoglu, T. S. Rahman, *Surf. Sci.* 600 (2006) 484.
- [28] H. Yildirim, A. Kara, T. S. Rahman, *Phys. Rev. B* 76 (2007) 165421.
- [29] G. Henkelman, H. Jónsson, *Phys. Rev. Lett.* 90 (2003) 116101.
- [30] F. Montalenti, Transition-path spectra at metal surfaces, *Surf. Sci.* 543 (2003) 141.
- [31] J. Jacobsen, K. W. Jacobsen, J. K. Norskov, *Surf. Sci.* 359 (1996) 37.
- [32] D. C. Rapaport, *The Art of Molecular Dynamics Simulation*, Cambridge University Press, 2004.
- [33] G. Ehrlich, F. G. Hudda, *J. Chem. Phys.* 44 (1039).
- [34] L. Schwoebel, *J. Appl. Phys.* 40 (614).
- [35] J. W. Evans, D. E. Sanders, P. A. Thiel, A. E. DePristo, *Phys. Rev. B* 41 (1990) R5410.
- [36] J. Frantz, M. Rusanen, K. Nordlund, I. Koponen, *J. Phys.: Condens. Matter* 16 (2004) 2995.
- [37] A. Einstein, *Ann. Phys. (Leipzig)* 17 (1905) 549 (English transl. *Investigations on the Theory of Brownian Movement*, Dover, New York, 1956).